Chiral Cyclopentadienyl Ligands as Stereocontrolling Element in Asymmetric C –H Functionalization

Baihua Ye and Nicolai Cramer

Science **338**, 504 (2012);
DOI: 10.1126/science.1226938

Science (print ISSN 0036-8075; online ISSN 1095-9203) is published weekly, except the last week in December, by the American Association for the Advancement of Science, 1200 New York Avenue NW, Washington, DC 20005.

Chiral Cyclopentadienyl Ligands as Stereocontrolling Element in Asymmetric C–H Functionalization

Baihua Ye and Nicolai Cramer*

Metal complexes coordinated by a single cyclopentadienyl (Cp) ligand are widely used, versatile catalysts, but their application to asymmetric reactions has been hindered by the difficulty of designing Cp substituents that effectively bias the coordination sphere. Here, we report on a class of simple C_2-symmetric Cp derivatives that finely control the spatial arrangement of the transiently coordinated reactants around the central metal atom. Rhodium(III) complexes bearing these ligands proved to be highly enantioselective catalysts for directed carbon-hydrogen (C–H) bond functionalizations of hydroxamic acid derivatives.

Since the discovery of ferrocene 70 years ago, cyclopentadienyl (Cp)–coordinated metal complexes contributed tremendously to the rise of organometallic chemistry. Countless transition-metal complexes have been prepared with Cp itself or its most popular pentamethylcyclopentadienyl analog (Cp*), and many of them are highly efficient catalysts for a broad range of transformations (*1*). Despite such favorable characteristics as stability and robustness, Cp ligands have been largely bypassed by other classes of ligands—such as diamines, phosphines, and carbenes—as carriers of chiral bias in asymmetric catalysis (*2*). The simple Cp or Cp* motif appears often in mixed-ligand designs comprising one or more additional coordination groups responsible for the chiral environment (*3*, *4*). However, only a few chiral Cp derivatives with non-coordinating substituents, and their corresponding metal complexes, have been synthesized (*5*–*11*), and they have rarely been applied as catalysts. With the exception of the Co(I)-catalyzed cyclotrimerizations reported by Heller, Hapke, and Gutnov (*12*–*14*), no notable chiral induction has been achieved with their respective late-transition metal complexes in catalytic reactions.

This discrepancy might derive from inherent difficulties linked to the design and synthesis of chiral Cp ligand derivatives. Although representing a long-standing problem in asymmetric catalysis, it has been systematically neglected. The striking opportunities inherent in addressing these shortcomings become clear by just considering half-sandwich complexes (*15*, *16*) with a d^6-electron count such as Cp Rh(III), Ir(III), Ru(II), and Co(I), which catalyze a range of important reactions (*17*–*23*). Often, these reactions require that, during the catalytic cycle, all three remaining coordination sites bind substrate(s) and reactants, leaving Cp as the sole permanent ligand on the metal. This characteristic makes the development of catalytic asymmetric versions enormously challenging because selectivity stems from the arrangement of the three other ligands around the central metal. Pseudotetrahedral complexes of the type $[(\eta^5\text{-}C_5H_5)ML^1L^2L^3]$ are chiral-at-metal (*24*, *25*), arising from a face-selective approach of the third ligand L^3 to the fluxional 16-electron intermediate, leading without a controlling element to a racemate.

Achieving high levels of stereoselectivity for this association is a key hurdle for successful asymmetric catalysis. The facial selectivity of the ligand association must be imposed by the chiral space crafted by an enantiopure Cp congener. We identified three criteria to design catalysts for an efficient enantioselective process: (i) use of C_2-symmetric Cp derivatives to avoid the complicating factor of diastereomer formation in coordination of the metal to either ligand face; (ii) restriction of rotation around the Cp moiety to lock in one of two substrate alignments, which must be highly preferred over the other, as this ratio reflects the maximum attainable selectivity; and (iii) steric blocking perpendicular to the Cp plane to induce approach of the incoming reactant R_C from just one side. Taking these constraining factors into account, we hypothesized that a 1,2-disubstituted Cp ligand would favor the two orientations of the small and large substrate parallel to the positional locks (S_S and S_L, structures **A** and **B**, Fig. 1). A

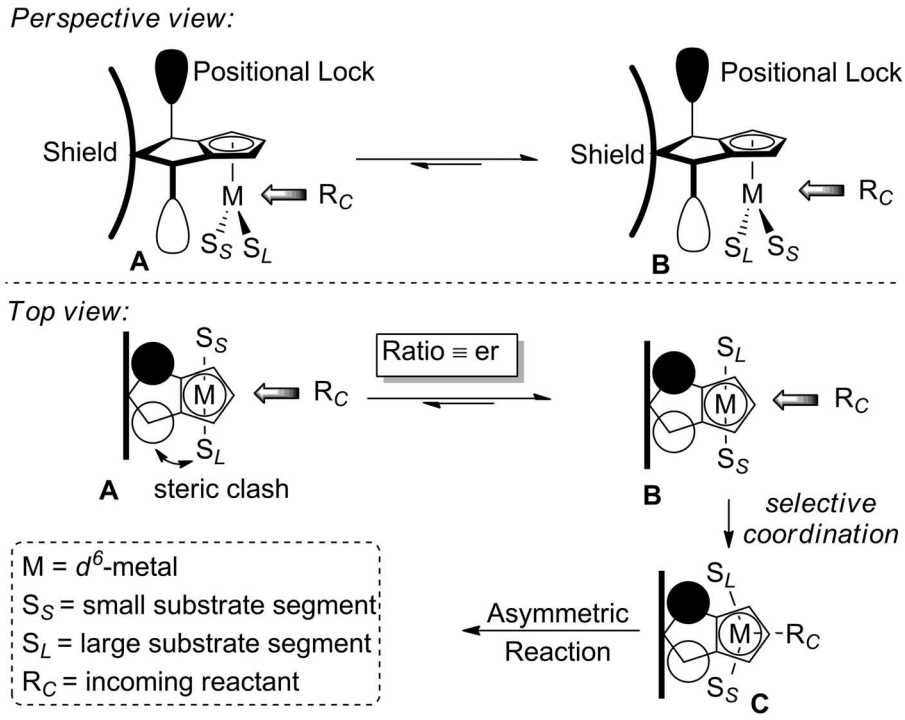

Fig. 1. Conceptual design of the chiral Cp^{x*} complexes.

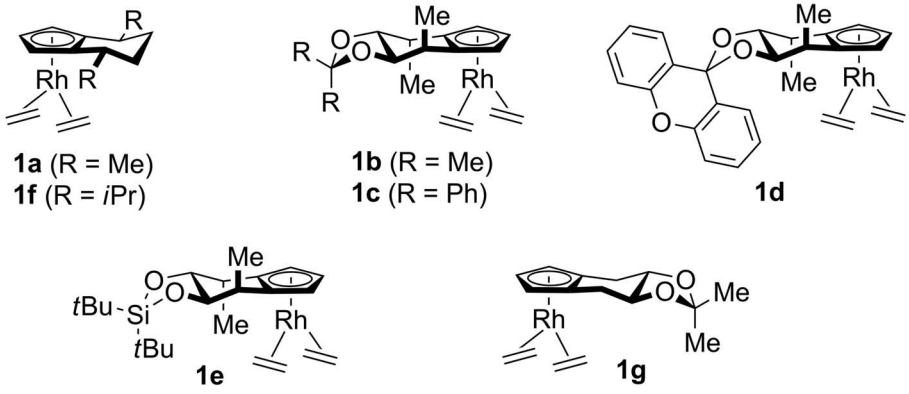

Fig. 2. Structure of the chiral $Cp^{x*}Rh(I)$ complexes **1a** to **1f**.

Ecole Polytechnic Fédérale de Lausanne, School of Basic Sciences, Institute of Chemical Sciences and Engineering, Laboratory of Asymmetric Catalysis and Synthesis, BCH 4305, CH-1015 Lausanne, Switzerland.

*To whom correspondence should be addressed. E-mail: nicolai.cramer@epfl.ch

bulky backbone should prevent the approach of the reactant R_C from the back. The C_2-symmetric chiral space, illustrated by the upward- and downward-oriented positional locks, should preferentially orient the larger ligand S_L away from the steric bulk and thus favoring conformer **B**. Association of R_C would lead then to **C** as a single diastereomer, competent for selective downstream reactions (*26*).

We prepared a range of rhodium(I) complexes (**1a** to **1g**, Fig. 2) with different backside shielding from the corresponding C_2-symmetric cyclopentadiene precursors (*27*). These Rh(I) complexes are relatively air-stable and easy to handle. In keeping with our interest in C–H bond functionalization using rhodium catalysts (*28*, *29*), we chose the Cp*Rh(III)-catalyzed C–H functionalization (*30*) of hydroxamic acid derivative recently reported by Fagnou (*31*) and Glorius (*32*) as an optimal reaction to challenge the viability of our concept. In situ oxidation of complex **1** with dibenzoylperoxide (DBPO) delivered directly a competent catalyst, presumably Rh(III) *bis*-benzoate complex **5** (*33*).

Complex **1g**, bearing only remote stereochemical substitution, displayed as expected only negligible selectivity (table S1, entry 1). Installing steric bulk closer to the Cp ring improved the enantiomeric ratio (er) to 73:27 (table S1, entry 2). Unexpectedly, when the methyl group was replaced with any larger substituent—e.g., an isopropyl group—the enantioselectivity dropped sharply (table S1, entry 3). We next evaluated the influence of the rigidifying *trans*-acetal group. With the two oxygen atoms being in *syn*-relation to both methyl groups of the cyclohexene, these are forced into the pseudo-axial position, increasing the bulk near the metal center and giving increased selectivity of 90:10 er (table S1, entry 6). In addition to this conformational effect, the acetal group protects the metal from backside approach by the olefin. Different larger groups were evaluated as well, and a benzophenone acetal moiety (**1c**) proved to be optimal, providing **4aa** with 92:8 er (table S1, entry 7).

We next turned our attention to the size of the acyl substituent R of the oxygen atom of the hydroxamate substrate, which we expected would influence the ratio of the two specific orientations of the cyclometalated intermediate **7**. Several acyl and carbonate derivatives were tested, and the readily accessible Boc-derivative (R=O*t*Bu) was optimal, giving complex **1c** 96:4 er (entry 10). The high solubility of the starting Rh(I) complex allowed a wide variation of solvents with conserved selectivity (entries 12 to 15), although the yields proved highest in ethanol. The catalyst loading could be lowered to 1 mole % without diminishing the reaction performance (entry 16). The activation proceeds even at 0°C with a slightly increased selectivity (entry 17).

The scope of the reaction was explored with the optimized catalyst **1c** and is outlined in Table 1. On the olefin acceptor side, a variety of styrenes are competent reaction partners, and the observed enantioselectivity is consistently excellent (Table 1, entries 1 to 7). Some structurally and electronically different terminal and cyclic olefins were tested, performing reliably, albeit in some instances with slightly reduced enantioselectivity (entries 8 to 13). Uniquely, vinyl trimethyl silane gives **4aj** with the opposite regioselectivity (>10:1, entry 9). The process is also general for the aryl hydroxamates **2a** to **2h** and different electronic and steric variations have little influence on yield and selectivity (entries 13 to 20).

The catalytic cycle of the reaction is presumably initiated by oxidation of the Cp^{x*}Rh(I) complex **1** by DBPO, giving **5** (fig. S4). Based on published mechanistic studies of the racemic version of this transformation (*31*, *34*), ligand exchange binds substrate **2a**, forming **6**. Cyclometalation by concerted metalation deprotonation mechanism and loss of benzoic acid leads to the crucial cyclometalated 16-electron species **7**. In the enantioselectivity-determining step, coordination of the olefin in a highly diastereoselective manner leads to 18-electron chiral-at-metal complex **8**, and its incorporation forms **10** (*35*). With the benzoic acid present in

Table 1. Substrate scope of the enantioselective activation/addition.

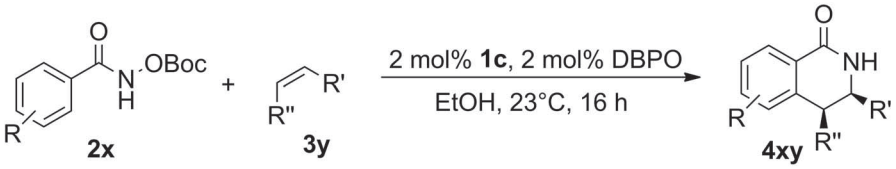

Entry	R	R'	R''	4	% yield*	er†
1	H	3-Me-C_6H_4	H	**4ab**	91	95 : 5
2	H	4-Me-C_6H_4	H	**4ac**	89	96 : 4
3	H	4-*t*Bu-C_6H_4	H	**4ad**	91	95.5 : 4.5
4	H	4-MeO-C_6H_4	H	**4ae**	88	96 : 4
5	H	4-F-C_6H_4	H	**4af**	87	95.5 : 4.5
6‡	H	4-CF_3-C_6H_4	H	**4ag**	81	95 : 5
7‡,‖	H	2-naphthyl	H	**4ah**	79	96.5 : 3.5
8‡	H	C≡C-TIPS	H	**4ai**	70	92 : 8
9‡	H	H	$SiMe_3$	**4aj**	74	85 : 15
10‡	H	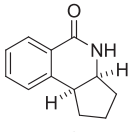		**4ak**	83	91 : 9
11	H	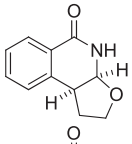		**4al**	81	93 : 7
12‡	H	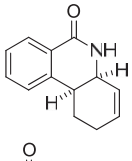		**4am**	59	91.5 : 8.5
13	3-Me	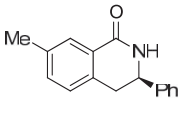		**4ba**	80	96 : 4
14	4-Me	Ph	H	**4ca**	85	97 : 3
15	4-MeO	Ph	H	**4da**	68	96.5 : 3.5
16‖	4-NO_2	Ph	H	**4ea**	76	96.5 : 3.5
17	4-Br	Ph	H	**4fa**	78	96.5 : 3.5
18	4-Cl	Ph	H	**4ga**	81	96.5 : 3.5
19	4-F	Ph	H	**4ha**	81	96 : 4
20		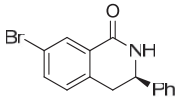 **4ia** 1 : 1.3 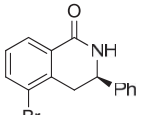 **4ia'**			83	95 : 5 (**4ia**) 88.5 :11.5 (**4ia'**)

* Isolated yields; † Determined by HPLC on a chiral stationary phase; ‡ with 5 mol% of **1c**; ‖ CH_2Cl_2 instead of EtOH.

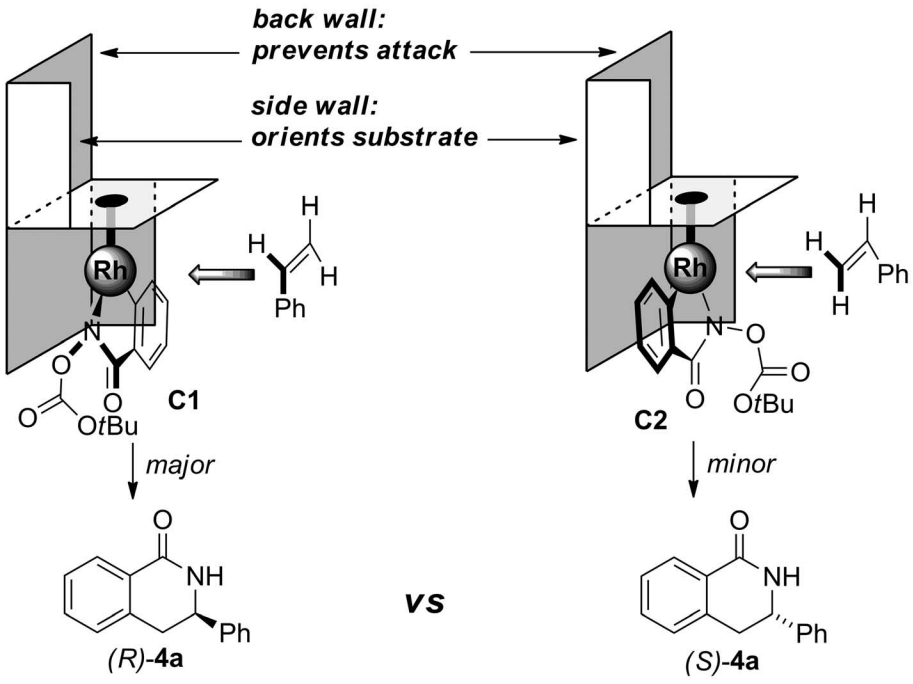

Fig. 3. Postulated model for the stereochemical preference with complex **1c**.

the reaction media, ligand exchange/protonation regenerates **5** and expels product **4** and *t*-butyl hydrogen carbonate, which collapses to CO_2 and *t*BuOH without changing the overall acidity of the medium during the course of the reaction. The absolute configuration of product **4a** was determined to be (*R*)-**4a** (*36*). The underlying selectivity of the reaction was visualized by a graphical model representing the complex **1c** (Fig. 3) (*37*). The back wall forces styrene to approach from the open face with the phenyl group oriented away from the Cp ring. Conformer **C1** having its hydroxamate moiety turned away from the steering side wall is the faster-reacting isomer, leading to (*R*)-**4a**.

In conclusion, we have described a class of chiral Cp^{x*} analogs with low molecular weight that desymmetrize a rhodium(III)-catalyzed directed C–H bond functionalization. The reaction proceeds under mild conditions and is high yielding and enantioselective. This development should become a stepping-stone to unlock the potential of chiral Cp analogs as steering ligands in enantioselective late-transition metal catalysis with half-sandwich complexes.

References and Notes

1. R. H. Crabtree, *The Organometallic Chemistry of the Transition Metals* (Wiley, New York, ed. 3, 2001).
2. E. N. Jacobsen, A. Pfaltz, H. Yamamoto, Eds., *Comprehensive Asymmetric Catalysis: Vol. I-III, Suppl. I-II,* (Springer, New York, 1999).
3. A. H. Hoveyda, J. P. Morken, *Angew. Chem. Int. Ed. Engl.* **35**, 1262 (1996).
4. U. Siemeling, *Chem. Rev.* **100**, 1495 (2000).
5. R. L. Halterman, K. P. C. Vollhardt, *Organometallics* **7**, 883 (1988).
6. R. L. Halterman, *Chem. Rev.* **92**, 965 (1992).
7. H. Schumann *et al.*, *Eur. J. Inorg. Chem.* **2002**, 211 (2002).
8. R. L. Halterman, L. D. Crow, *Tetrahedron Lett.* **44**, 2907 (2003).
9. A. Gutnov, B. Heller, H.-J. Drexler, A. Spannenberg, G. Oehme, *Organometallics* **22**, 1550 (2003).
10. A. Gutnov, H.-J. Drexler, A. Spannenberg, G. Oehme, B. Heller, *Organometallic* **23**, 1002 (2004).
11. G. P. McGlacken, C. T. O'Brien, A. C. Whitwood, I. J. S. Fairlamb, *Organometallics* **26**, 3722 (2007).
12. A. Gutnov *et al.*, *Angew. Chem. Int. Ed.* **43**, 3795 (2004).
13. B. Heller *et al.*, *Chemistry* **13**, 1117 (2007).
14. M. Hapke *et al.*, *J. Org. Chem.* **75**, 3993 (2010).
15. Sandwich complexes containing two Cp moieties such as *ansa*-ebthi metallocenes of Ti, Zr, or Hf are versatile catalysts for several asymmetric reactions. For an overview, see (*16*).
16. A. H. Hoveyda, J. P. Morken, *Angew. Chem. Int. Ed. Engl.* **35**, 1262 (1996).
17. C. P. Lenges, M. Brookhart, *J. Am. Chem. Soc.* **119**, 3165 (1997).
18. H. Chen, S. Schlecht, T. C. Semple, J. F. Hartwig, *Science* **287**, 1995 (2000).
19. J. F. Hartwig *et al.*, *J. Am. Chem. Soc.* **127**, 2538 (2005).
20. B. M. Trost, M. U. Frederiksen, M. T. Rudd, *Angew. Chem. Int. Ed.* **44**, 6630 (2005).
21. A. H. Roy, C. P. Lenges, M. Brookhart, *J. Am. Chem. Soc.* **129**, 2082 (2007).
22. A. D. Bolig, M. Brookhart, *J. Am. Chem. Soc.* **129**, 14544 (2007).
23. M. Zhou, N. D. Schley, R. H. Crabtree, *J. Am. Chem. Soc.* **132**, 12550 (2010).
24. H. Brunner, *Angew. Chem. Int. Ed.* **38**, 1194 (1999).
25. E. B. Bauer, *Chem. Soc. Rev.* **41**, 3153 (2012).
26. Although Fig. 1 depicts solely the differences of the two most stable conformers, we assume that reactions proceed under Curtin-Hammett conditions. Therefore, no judgment on the reactive conformer, the one with a lower transition state, is possible.
27. Materials and methods are available as supplementary materials on *Science* Online. For the syntheses and an x-ray structure of **1c**, see figs. S1 to S3.
28. D. N. Tran, N. Cramer, *Angew. Chem. Int. Ed.* **49**, 8181 (2010).
29. D. N. Tran, N. Cramer, *Angew. Chem. Int. Ed.* **50**, 11098 (2011).
30. G. Song, F. Wang, X. Li, *Chem. Soc. Rev.* **41**, 3651 (2012).
31. N. Guimond, S. I. Gorelsky, K. Fagnou, *J. Am. Chem. Soc.* **133**, 6449 (2011).
32. S. Rakshit, C. Grohmann, T. Besset, F. Glorius, *J. Am. Chem. Soc.* **133**, 2350 (2011).
33. Related Cp*Rh(III) *bis*-carboxylate complexes are most likely the active catalytic species in the racemic reaction and are usually generated in situ from $\{[Cp^*Rh(Cl_2)]_2\}$ by silver salts and carboxylate additives.
34. D. Lapointe, K. Fagnou, *Chem. Lett.* **39**, 1118 (2010).
35. L. Xu, Q. Zhu, G. Huang, B. Cheng, Y. Xia, *J. Org. Chem.* **77**, 3017 (2012).
36. F. A. Davis, Y. W. Andemichael, *J. Org. Chem.* **64**, 8627 (1999).
37. J. A. Gladysz, B. J. Boone, *Angew. Chem. Int. Ed. Engl.* **36**, 550 (1997).

Acknowledgments: This work is supported by the European Research Council (ERC) under the European Community's Seventh Framework Program (FP7 2007–2013)/ERC Grant agreement 257891. We thank R. Scopelliti for x-ray crystallographic analysis of **1c**. CCDC 898196 contains the crystallographic data for **1c**. These data can be obtained free of charge from the Cambridge Crystallographic Data Centre, www.ccdc.cam.ac.uk/data_request/cif.

Supplementary Materials

www.sciencemag.org/cgi/content/full/338/6106/504/DC1
Materials and Methods
Figs. S1 to S3
References (*38*–*43*)

4 July 2012; accepted 10 September 2012
10.1126/science.1226938

Fluorescence Enhancement at Docking Sites of DNA-Directed Self-Assembled Nanoantennas

G. P. Acuna,* F. M. Möller, P. Holzmeister, S. Beater, B. Lalkens, P. Tinnefeld*

We introduce self-assembled nanoantennas to enhance the fluorescence intensity in a plasmonic hotspot of zeptoliter volume. The nanoantennas are prepared by attaching one or two gold nanoparticles (NPs) to DNA origami structures, which also incorporated docking sites for a single fluorescent dye next to one NP or in the gap between two NPs. We measured the dependence of the fluorescence enhancement on NP size and number and compare it to numerical simulations. A maximum of 117-fold fluorescence enhancement was obtained for a dye molecule positioned in the 23-nanometer gap between 100-nanometer gold NPs. Direct visualization of the binding and unbinding of short DNA strands, as well as the conformational dynamics of a DNA Holliday junction in the hotspot of the nanoantenna, show the compatibility with single-molecule assays.

Single-molecule fluorescence measurements report on kinetic processes without the need for synchronization, lifetimes of intermediates, structure, stoichiometry of subpopulations, and the choreography of biomolecular processes (*1*, *2*). Yet, only a small number